



ISSN: 1813-162X (Print); 2312-7589 (Online)

Tikrit Journal of Engineering Sciences

available online at: <http://www.tj-es.com>

TJES

Tikrit Journal of  
Engineering Sciences

# Flexural Behavior of a Composite Concrete Castellated Double Channel Steel Beams Strengthening with Reactive Powder Concrete

Nihad Yaseen Abbas \*, Ahmad Jabbar Hussain Alshimmeri 

Civil Engineering Department, College of Engineering, University of Baghdad, Baghdad, Iraq.

**Keywords:**

Castellated; Composite beam; Deflection; Experimental test; Lacing reinforcement; Strengthening.

**Highlights:**

- Structural performance of using a 2C hot rolled as castellated steel beams.
- Experimental use of lacing and RPC to strengthen castellated beams.
- Performance of neglected welding the strengthening castellated beams.

**ARTICLE INFO****Article history:**

Received	03 July	2023
Received in revised form	19 Sep.	2023
Accepted	28 Sep.	2023
Final Proofreading	24 Nov.	2023
Available online	12 Apr.	2024

© THIS IS AN OPEN ACCESS ARTICLE UNDER THE CC BY LICENSE. <http://creativecommons.org/licenses/by/4.0/>

**Citation:** Abbas NY, Alshimmeri AJH. Flexural Behavior of a Composite Concrete Castellated Double Channel Steel Beams Strengthening with Reactive Powder Concrete. *Tikrit Journal of Engineering Sciences* 2024; 31(2): 28-42. <http://doi.org/10.25130/tjes.31.2.4>

**\*Corresponding author:****Nihad Yaseen Abbas**

Civil Engineering Department, College of Engineering, University of Baghdad, Baghdad, Iraq.

**Abstract:** This paper examines the experimental flexural performance of the strengthening composite concrete asymmetrical castellated steel beam of double channel shape by connecting two castellated hot rolled steel channels back-to-back using bolts along its length to obtain a built-up I-shaped form with a new total beam depth heightened by 52.4%. This research tested four specimens: the first was a reference specimen without any strengthening techniques; the second was strengthened with RPC (Reactive Powder Concrete) in the steel web region; the third was strengthened by RPC reinforced with a lacing rebar. Also, this study investigated the welding effects in web posts for the top and bottom parts of the castellated steel in the fourth specimen. All specimens were tested under simply supported conditions by applying two-point static loads on the concrete deck slab of the composite beams. The ultimate load deflection, stiffness, ductility, energy absorption capacity, and failure mode were investigated and discussed. According to the experimental results, the ultimate load capacity increased 24.01% and 48.34% in the second and third specimens, respectively, with increased stiffness, ductility, and energy absorption capacity compared with the first specimen. In contrast, the ultimate load capacity decreased by 11.02 % in the fourth specimen (strengthening without welding in web posts), reducing stiffness and ductility compared with the first specimen (reference).

## أداء الانحناء للعتبات المركبة من الخرسانة وقلعوية مزدوج حديد الساقية والمقواة بالمساحيق الخرسانية الفعالة

نهاد ياسين عباس، أحمد جبار حسين الشمري

قسم الهندسة المدنية / كلية الهندسة / جامعة بغداد / بغداد – العراق.

### الخلاصة

يفحص هذا البحث عملياً أداء الانحناء للعتبات المقواة والمركبة من الخرسانة ومقاطع الحديد القلعوية المزدوجة القياسية على شكل ساقية مربوطة بأخرى مماثلة في منطقة الجذع عن طريق الظهر باستعمال عدد من البراغي على طول المقطع لتشكيل مقطع مركب يشبه الحرف I. يتم زيادة العمق الاجمالي للعتبة بنسبة ٤٠,٤٪. في هذا البحث تم فحص أربع عينات: النموذج الاول هو نموذج مرجعي بدون اي تقنيات للتقوية والنموذج الثاني كانت التقوية فيه بالمساحيق الخرسانية الفعالة في منطقة الجذع اما النموذج الثالث فكان التقوية بالمساحيق الخرسانية الفعالة وبحديد التسليح. فضلاً عن دراسة تأثير اللحام على مناطق اتحاد المقطعين العلوي والسفلي للحديد القلعوي في النموذج الرابع والمقوى بالمساحيق الكونكريتية الفعالة مع حديد تسليح لكن بدون لحام كل النماذج كانت بنفس الظروف من الدعم البسيط مع تسليط حملين مركزيين على سطح السقف الخرساني للعتبة المركبة. التحمل الاقصى والهطول والصلابة والمطيلية وسعة امتصاص الطاقة وشكل الفشل النهائي قد تم قياسها ومناقشة نتائجها. واستناداً الى الفحص المخبري فإن هناك زيادة بالتحمل الاقصى في النموذجين الثاني والثالث بنسبة ٢٤,٠١٪ و ٤٨,٣٤٪ على التوالي مع زيادة بالصلابة والمطيلية وسعة امتصاص الطاقة وعلى النقيض من ذلك هناك نقص في التحمل الاقصى بحوالي النموذج الرابع المقوى بدون لحام في مناطق الجذع مع نقصان في الصلابة والمطيلية مقارنة بالنموذج الاول (المرجع).

**الكلمات الدالة:** القلعوي، العوارض المركبة، الانحراف، الاختبار التجريبي، تقوية الربط، التقوية.

### 1. INTRODUCTION

Structural engineers constantly control the behavior and geometry of steel structures to attain lighter weight, cheaper construction, and higher strength. One such advancement in built-up structural components involved castellated steel beams to modify hot-rolled I, H, or U steel sections by zigzagging the webs longitudinally, separating the two halves, and connecting the two sections. When the depth of all I-beams increases up to 50%, the structure's flexural strength is greatly improved due to the increase in the beam plastic section modulus. During construction, the beam depth increases, which improves the castellated beam's stiffness and strength [1, 2]. Larnach and Park [3] investigated the composite effect of castellated girders and concrete deck slabs by testing six distinct castellated composite T-girders under extreme shear loads. The samples were made from universal sections, and the top concrete flange was attached to the steel beam via spiral shear connections. The beams were subjected to various point loads. The collapse was caused by the buckling of the inner web panels and the fracture of the concrete flange bottom. Unexpectedly, a segment with a solid web had a lower-appearing neutral axis position than a component with a web opening. Usually, concrete and steel are joined to create composite beams, which effectively utilize the benefits of both sections. When concrete confinement supports castellated beams, composite components, such as steel-encased steel web, increase the segment's maximum load capacity and heap conveying limit, increasing the structure's fire resistance [4]. Hadeed and Alshimmeri [5] investigated the reinforced noncomposite castellated IPE steel beams with high-strength concrete and steel-laced reinforcement with and without welding between two parts of the steel web, increasing the ultimate load capacity of approximately

49.86% to 106.44% for the strengthened beam compared to a reference beam. Reactive Powder Concrete (RPC) is a cementation material used in the reinforced concrete mix or as an overlay to improve the mechanical and chemical properties. It has gained much attention due to its high-strength performance in civil, petroleum, nuclear, municipal, marine, and military buildings, among other projects [6-8]. Ammar and Alshimmeri [9] experimentally studied the enhancement of the load-carrying capacity of asymmetrical castellated beams (rolled standard section IPE 140 was used as a root section) with encasement by Reactive Powder Concrete (RPC) with lacing reinforcement at the steel web. The authors also studied the effect of the gap between the top and bottom parts of asymmetrical castellated steel beams at the web post regions. The researchers presented two concentrated load test results for four specimens. The first specimen was unstrengthened as a reference, while the second, third, and fourth specimens were strengthened with RPC, lacing, and deference gaps by about (19.1 mm, 38.2 mm, and 57.3 mm), respectively. The results showed a deflection decrease of about 33.33%, 52.77%, and 27.78%, with ultimate load capacity increase of about 26.92%, 46.15%, and 9.23%, respectively, compared with the reference specimen. The only difference among these samples was the gap between the upper and lower parts of the castellated steel beam. Therefore, increasing the gap increased the capacity to carry the load. Khaleel and Al-Shamaa [10] studied five specimens of 2C-shape beams with different shapes and numbers of openings web. This study showed that bearing strength decreased when the web holes were few. The bearing strength increased as the number of web holes increased to a

specific limit. Also, if openings exceeded a specific limit, the bearing force decreased. The increase rate in the bearing force was between 17.7% to 40.0%. Al-Tameemi and Alshimmeri [11] experimentally studied asymmetrical, castellated composite concrete beams made of IPE steel and RPC. Compared to the reference composite castellated beam (without strengthening), they found that the ultimate load capacity of the beams enhanced by roughly 10.5% to 19.5%. According to a literature survey, no theoretical or experimental investigations have examined the behavior of the asymmetrical composite concrete castellated steel beams (two steel channels joined back-to-back by bolts). The primary objective of this experimental study is to investigate the behavior of composite concrete asymmetrical castellated steel beams (double channel shape connected back-to-back by bolts) strengthening with RPC without and with steel rebar's lacing reinforcement. Also, to study the effectiveness of the welding between two parts of the castellated steel web, the resulting product was compared with a reference specimen (without strengthening). The ultimate load, deflection, stiffness, ductility, and energy absorption capacity were studied and discussed in the present experimental research.

**2. MATERIALS AND METHODS**

**2.1. Specifications**

In the experimental part, four specimens were designed as asymmetrical double-rolled castellated steel channel sections (2C7×12.25) and (2C8×13.75) [12] connected back-to-back by bolts. Specimens were tested with a clear span length (3100 mm) and a four-point load

setup, including support points. The specimens' details and their strengthening techniques are illustrated in Table 1 and Figs. (1-4).

**Table 1** Details of the Tested Specimens Used in Experimental Work.

Spec. No.	Spec. Symbol *	Description of Specimens
1	CACB <sub>2</sub> C/ R	Asymmetrical composite concrete-castellated steel beam (double channel shape connected back-to-back by bolts), the top half of (2C7×12.25) and the bottom half of (2C8×13.75) welded in the web posts (Ref.).
2	CACB <sub>2</sub> C -r	Asymmetrical composite concrete-castellated steel beam (double channel shape connected back-to-back by bolts), the top half of (2C7×12.25) and the bottom half of (2C8×13.75) welded in the web posts with RPC, incased the web.
3	CACB <sub>2</sub> C- rL	Asymmetrical composite concrete-castellated steel beam (double channel shape connected back-to-back by bolts), the top half of (2C7×12.25) and the bottom half of (2C8×13.75) welded in the web posts with RPC and Lacing, on the web.
4	CACB <sub>2</sub> C- rLG0%	Asymmetrical composite concrete-castellated steel beam (double channel shape connected back-to-back by bolts), the top half of (2C7×12.25) and the bottom half of (2C8×13.75) without welded (gap =0 mm) in the web posts, with RPC and Lacing bars on the web.

Where A=asymmetrical, C= composite beam, CB= castellated beam, 2C= Double Steels Channels shape connected back-to-back by bolts, L= lacing (reinforcement bar =6 mm), R= reference beam, r= reactive powder concrete in steel web, and G= gap space between post web of castellated two steels channels shapes (without welding).

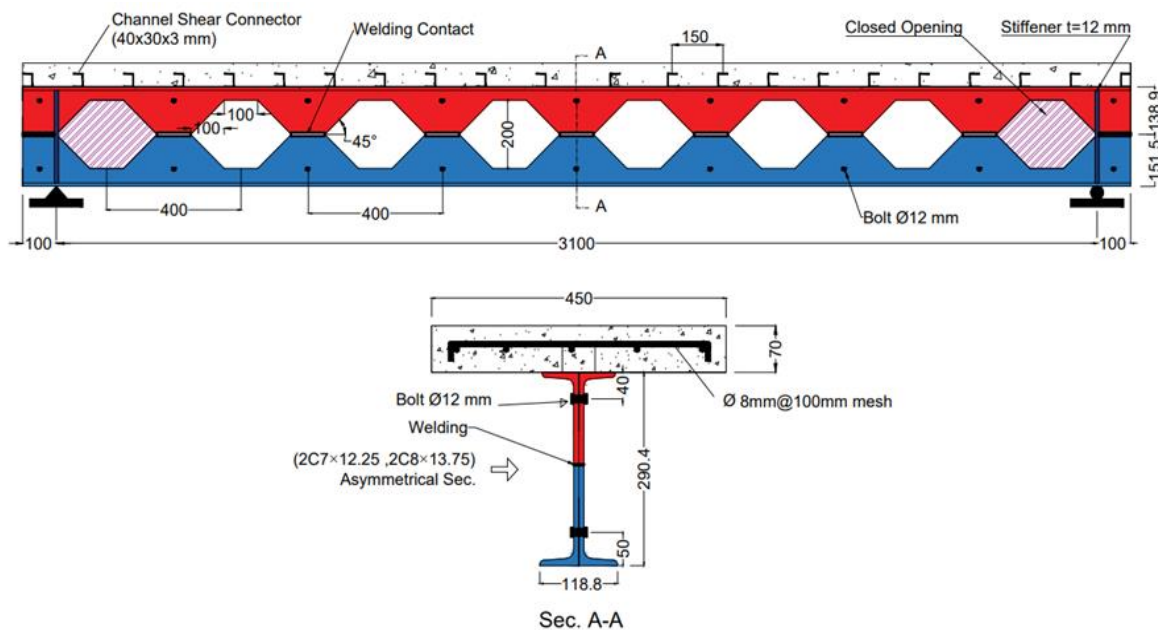


**Fig. 1** No. 1 (CACB<sub>2</sub>C/R) Specimen Details, All Dimensions in mm.

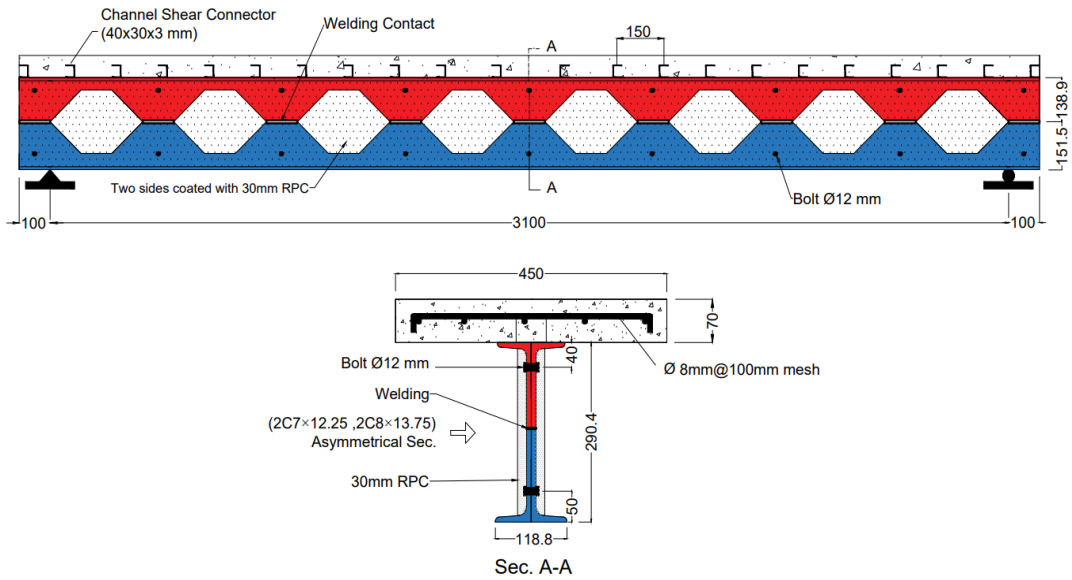


**Fig. 2** No. 2 (CACB2C- r) Specimen Details, All Dimensions in mm.

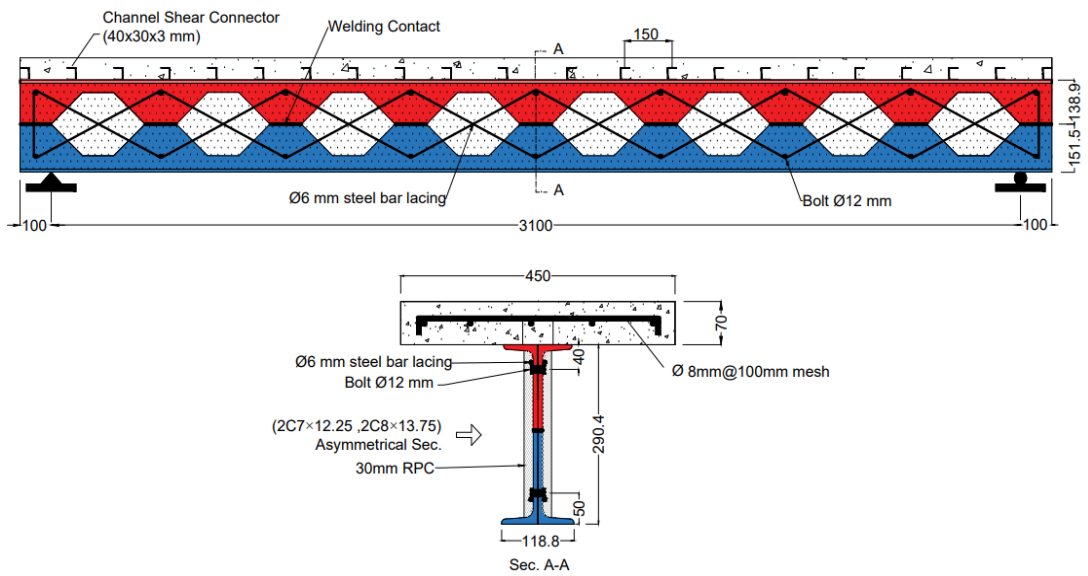


**Fig. 3** No. 3 (CACB2C- rL) Specimen Details, All Dimensions in mm.

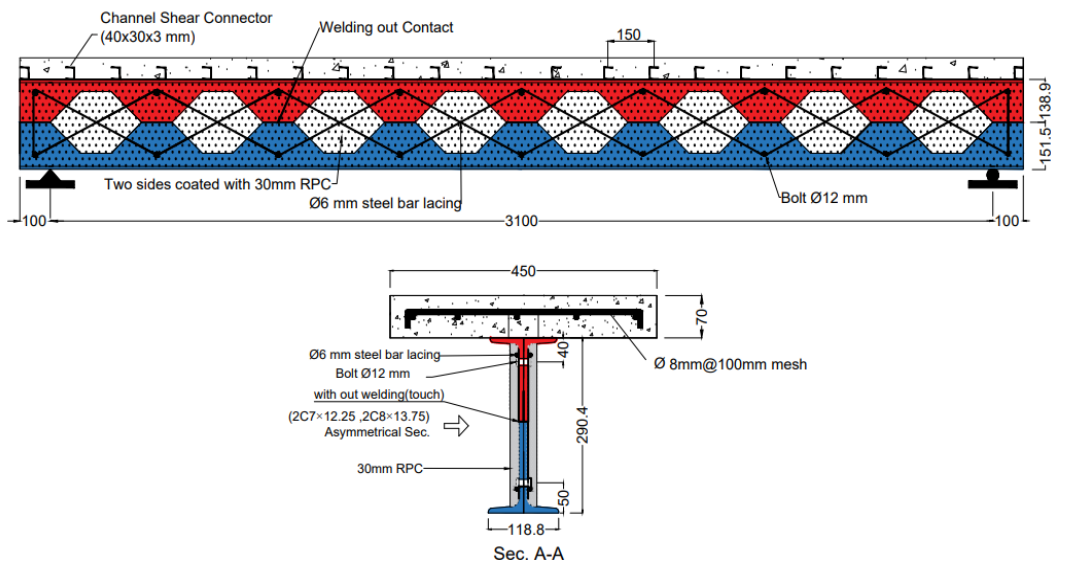


**Fig. 4** No. 4 (CACB2C- rL G 0%) Specimen Details, All Dimensions in mm.



**2.2. Steel**

According to the Steel Design Guide-31 restrictions [1], a double hot rolled steel channel shape (2C712.25) and (2C813.75) was designed and fabricated for making an asymmetrical steel beam used for the root section to fabricate four specimens of castellated steel beams, as shown in Fig. 5 and Table 2. The fabrication was done by cutting the web longitudinally in a zigzag line around the line in the mid-web section. The cutting process was conducted using a Computer Numerical Control (CNC) machine to achieve the precise opening shape. The two halves of the steel channel shape were separated, moved, and then welded back together in web posts using a 3mm thickness welding rod to form a castellated channel steel section. As shown in Fig. 6 [13] and Fig. 7, the castellated double steel channel beam was constructed by bolting two channels together at a 52.4% higher height than the root

section, which gives the new segment a greater part module and stronger bending rigidity than the root roll. It is worth mentioning that using a double channel shape (2C) to form a castellated steel beam gives more freedom in the cutting direction and formation during the castellation process. Therefore, there were no cutting losses at the castellated beam edges compared to forming an I section. Additionally, other steel components were used in this study, including the steel channels for shear connectors, the reinforcement of the slab, the rebar lacing, stiffeners, and bolts and nuts for connecting the double steel channels back-to-back. Fig. 8 and Table 3 illustrate the properties of stiffeners, shear connectors, steel beam coupons, reinforcement bars, and rebar lacing, tested specimens according to ASTM (2016) [14]. Hex bolts and nuts mechanical properties had a diameter of 12mm and  $f_u=800$  MPa, and  $f_y=640$  MPa, according to (BS 3692 Grade 8.8).

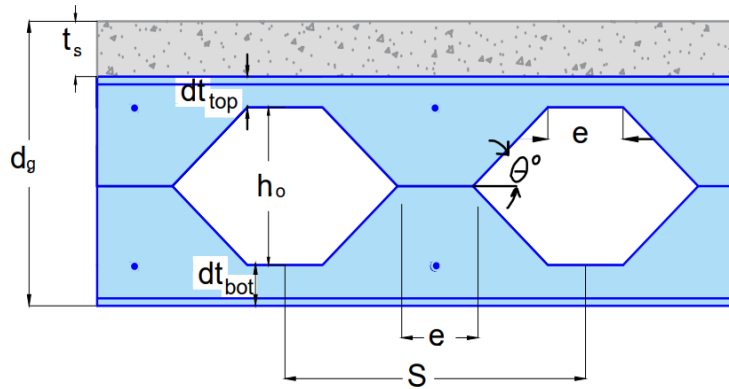


**Fig. 5** Denoted Dimensions of Castellated Specimens.

**Table 2** Steel Castellated Details of Specimens.

Spec. No.	$d_g$ mm	$d_{t\ top}$ mm	$d_{t\ bot}$ mm	$e$ mm	$S$ mm	$h_o$ mm	$\theta^\circ$	$t_s$ mm	$B_{eff}^*$ mm
1,2,3,4	360.4	38.9	51.5	100	400	200	45	70	450

\*Beff: effective width of deck slab.

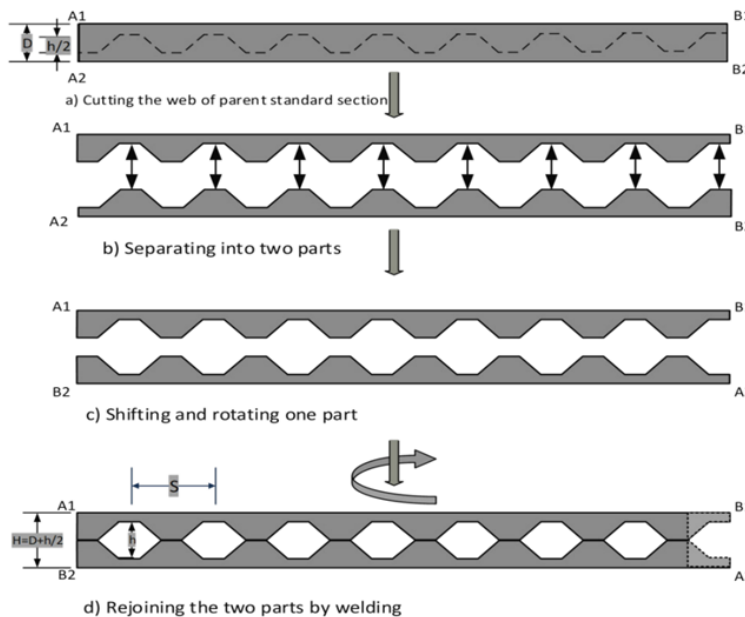
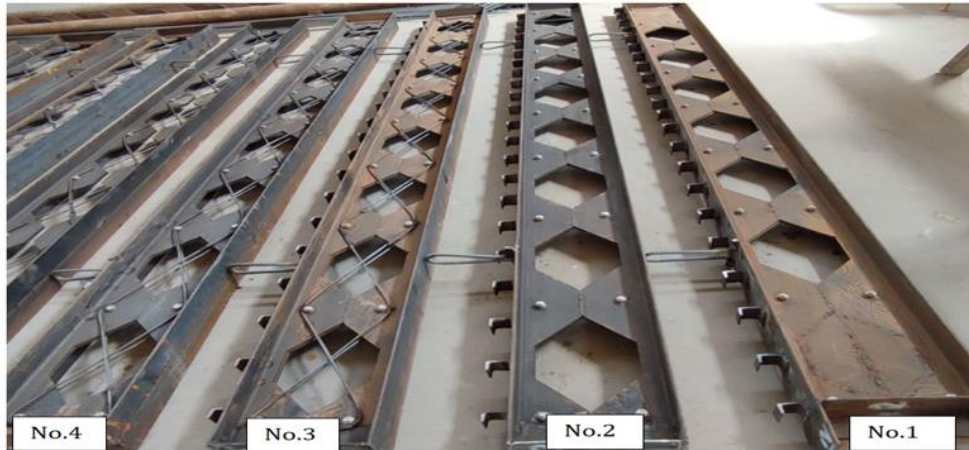


**Fig. 6** Manufacturing Method of the Castellated Steel Beam [12].



(a) Cutting by (CNC) plasma machine. (b) formation of the castellated steel beam.



(c) Finishing of constructing the castellated steel beams.

**Fig. 7** Fabrication of Castellated Double Steel Channel Beams.

**Table 3** Steel's Mechanical Properties.

Sample	Thickness (mm)	Yield Stress (MPa)	Ultimate Stress (MPa)	Elongation %	
				Tested Values	Recommended Values for Grade (ASTM-A370)
C7×12.25 (Web)	7.9	381	574	22	≥10
(flange)	9.29	340	585	22	≥10
C8×13.75 (Web)	7.9	390	621	24	≥10
(flange)	9.9	396	554	22	≥10
Stiffeners	12	390	621	24	≥10
Shear connectors	3	456	615	23.5	≥10
Reinforcement of Slab	(8 mm) diameter	420	623.5	20.3	≥10
Rebar Lacing	(6 mm) diameter	430	640	18	≥10



**Fig. 8** The Steel Materials: A. Shear Connectors, Lacing, and Bolts, B. Deck Slab Reinforcement.



**2.3. Concrete**

**2.3.1. Normal Concrete**

The concrete, mixed Type (I) cement, crushed gravel with a maximum aggregate size of 12 mm, and river fine sand were used to cast a deck slab of 7 cm in depth, 45 cm in width, and 330 cm in length. The weight ratios of the aggregate, sand, and cement were (1:1.5:3), and the water-to-cement ratio was 0.45. The target of the cube's compressive strength test result was (36

MPa), and the concrete compressive strength was assessed using standard cubes (150 x 150 x 150 mm) and cylinders (100 x 200 mm) taken from each specimen [15]. For all instances, a horizontal concrete deck was cast in wooden forms. The conventional cubes, cylinders, prisms, and the sides of the deck slab were removed from the molds a day after casting and covered in wet materials, as shown in Table 4 and Fig. 9.

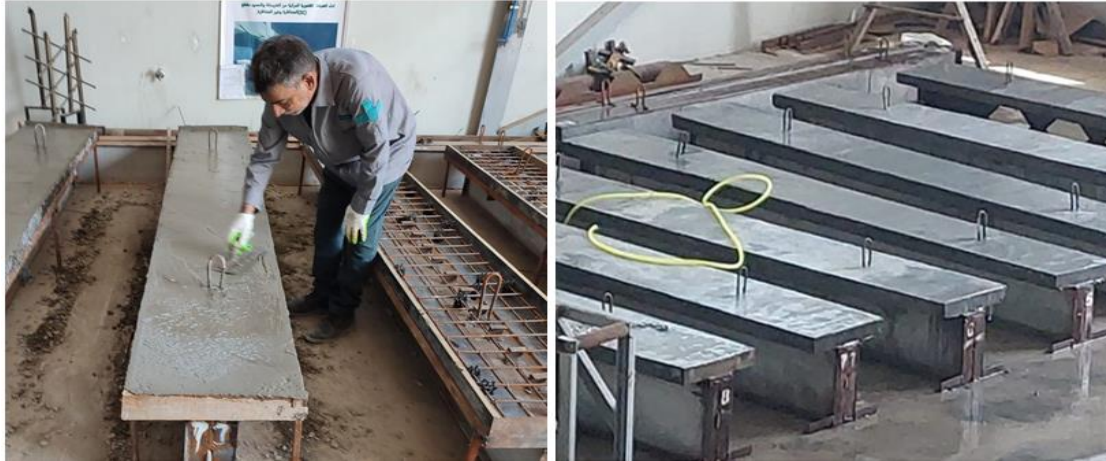


**Fig. 9** Casting and Curing of Specimens.

**Table 4** Mix Proportions for 1 m<sup>3</sup> of Concrete and RPC.

Type of Concrete	Cement Kg/m <sup>3</sup>	Sand Kg/m <sup>3</sup>	Gravel Kg/m <sup>3</sup>	Silica Fume Kg/m <sup>3</sup>	Steel Fiber Kg/m <sup>3</sup>	Water L/m <sup>3</sup>	W/C	Superplasticizer L/m <sup>3</sup>
NC	420	630	1260	0.0	0.0	190	0.45	3.5
RPC	955	1051	0.0	229	95	171	0.18	19

**2.3.2. Reactive Powder Concrete (RPC)**

To evenly distribute the silica fume particles among the cement particles, the silica fume and cement were combined in a rotary mixer for about three minutes in the dry state before adding the sand and mixing for an additional five minutes. The superplasticizer was dissolved in water. As the combination was mixed, the water and superplasticizer solution were progressively added. The entire mixture was then combined for three minutes. In three minutes, the fibers were evenly incorporated into the mixture. Then, the mixture was mixed for another two minutes. When the water was added to the mixture, one batch must be well-mixed [15]. Following the preparation of all specimens, the RPC for specimens was cast horizontally in wooden forms with a 30 mm thickness covering about two sides of the web. The specimen was dried with air once the moist materials were removed before testing. Standard cubes, cylinders, and prisms were cast and then cured for 28 days before being tested for compressive strength, splitting tensile strength, flexural tensile strength, and toughness using cubes and cylinders of various sizes (100 mm and 100 x 200 mm, respectively). The RPC mixes utilized are fully described in Table 4 and Fig. 10.



**Fig. 10** Casting RPC specimens.

The concrete materials were tested according to Iraq Standard Specifications (IQS) No. 45/1984 [16]. The mechanical characteristics of hardened RPC and standard hardened concrete are listed in Table 5.

**Table 5** Mechanical characteristics of normally hardened concrete and RPC.

Type of concrete	$f_c'$ (MPa)	$f_{cu}$ (MPa)	$f_c'/f_{cu}$	$f_{ct, test}$ (MPa)	$f_r, Test$ (MPa)	$E_c, test$ (MPa)
NC	26.64	33.3	0.8	3.11	3.31	23991
RPC	70.8	84.28	0.84	12.11	10.54	45525.9

**2.4. Testing Configurations**

All samples were evaluated using the hydraulic test device with a load cell (1000 kN maximum capacity). Each beam was subjected to two concentrated loads translated from the load distributor and loaded to failure in a monotonic manner. The specimens were similarly supported and loaded. Simple rollers held the model beams at a distance of 0.100 meters from the ends, and steel plates served as lateral stiffeners on each side of the supported specimen. The specimen was isolated at the two supports and the two concentrated loads positions using a rubber pad (100 mm width and 10 mm thickness) to ensure that the load was distributed evenly under the two concentrated loads and the upper two reactions. The two concentrated loads were placed at 0.95 m from the supports with steel plate setting, 100 mm wide and 10 mm thick. Three Linear Variable Differential Transformers (LVDT), a type of electrical transformer used to measure linear

displacement, were positioned beneath the beams' bottom surface at distances of 0.5166 m, 1.033 m, and 1.550 m from a single support (see Fig. 11). Additionally, two distinct strain gauge types were employed for the steel used model (FLA-6-11) with length=6mm and gauge factor =4; the steel strain gauges setting locations were in the bottom steel flange, lower steel web post welded, upper steel web post welded, and in the top steel flange. While model (PL-60-11) was used for concrete material with length=60mm and gauge factor =3. The concrete strain gauges setting locations were in the middle on the top surface and bottom surface of the concrete deck slab and in the mid surface of RPC. Before attaching the strain gauges, the steel and concrete surfaces were first smoothed, polished, and cleaned. The strain gauge was glued to ensure perfect contact using adhesive materials type CN-Y for steel and CN-E for concrete, see Figs. 11 and 12. Fig. 12 depicts a sketch of the test apparatus and associated instruments.

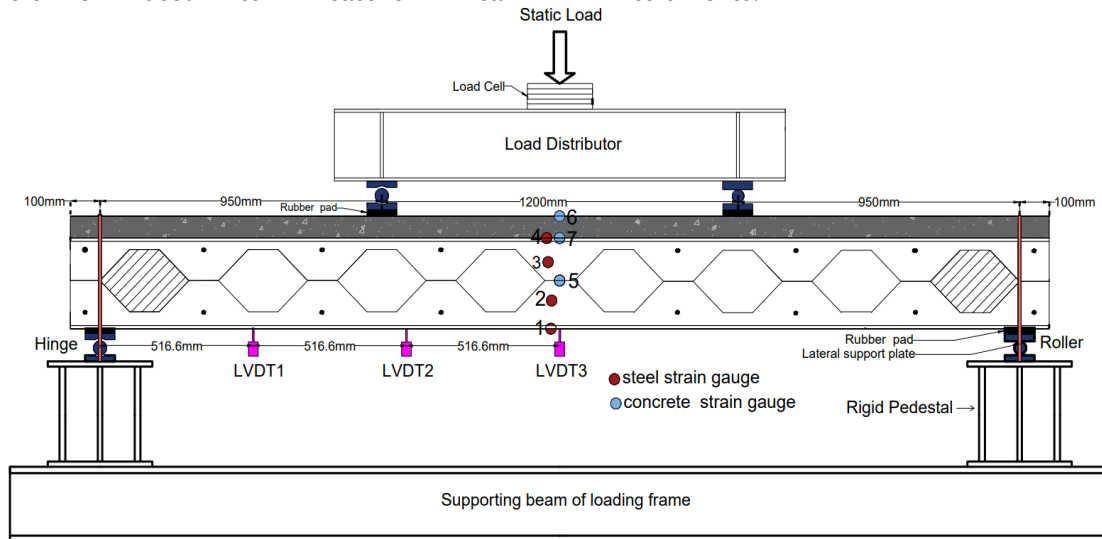


**Fig. 11** Testing Configurations of the Tested Specimens.

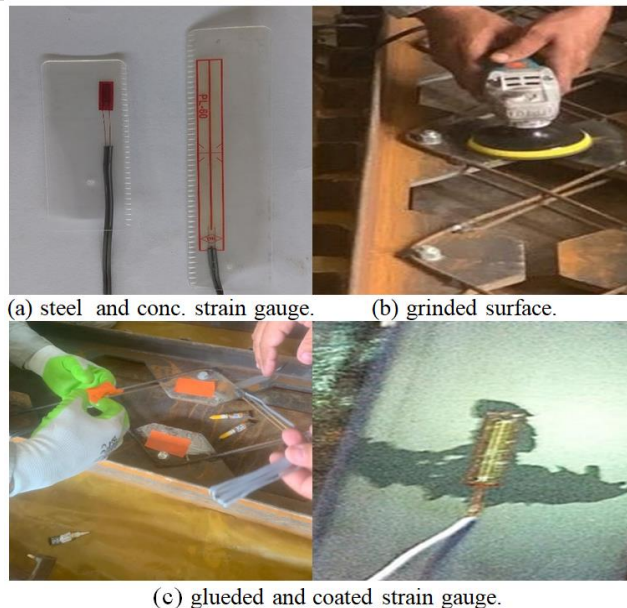


**Fig. 12** The Types of Strain Gauges, Grinded Surface, Glued, and Coated.





**Fig. 13** Data Logger Connected to a Computer.

The test machine with all attached instrumentations is shown in Fig. 14.

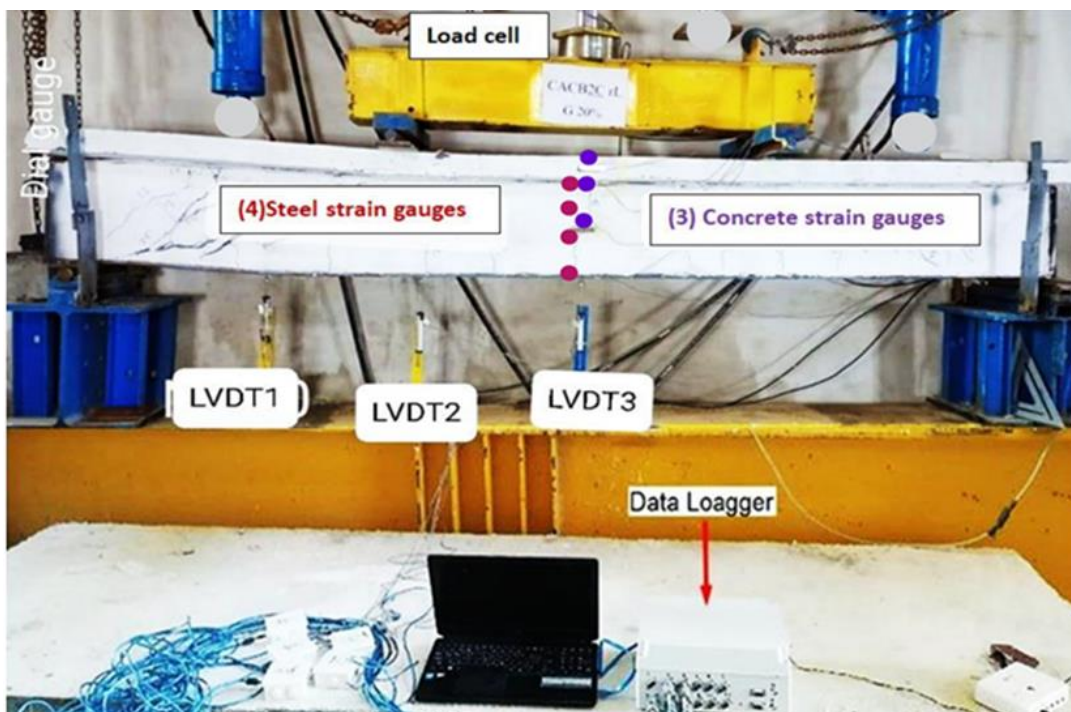


**Fig. 14** Test Setting Machine Supplied with All Instrumentations.

### 3. RESULTS AND DISCUSSION

#### 3.1. Deflection and Ultimate Load

Figure 15 illustrates the tested specimens' performance Nos. (1-4), as a deflected shape along the specimens' length at ultimate load capacity. As illustrated in Table 6 and Figs. 16 and 17, the deflection increased about 7%, 47%, and 5.7% in specimens Nos. (2-4) compared to reference specimen No.1. There is also a difference in an ultimate load of about +24.01%, +48.34%, and -11.02% in specimens Nos. (2-4), respectively, compared to reference specimen No.1. These results differ due to the effect of stiffness and ductility using strengthening techniques represented by RPC, lacing, and welding in the web posts region.

Table 7 illustrates the specimens' deflections at mid-span measured at level with an ultimate load of 341.70 kN and deflection of 12.26 mm of No.1 (CACB2C/R) as the reference specimen, as shown in Fig. 16. It was noted for specimen No.2 (CACB2C-r), the deflection decreased by 20.96%, and for specimen No.3 (CACB2C-rL) the deflection decreased by 24.87%. These deflection decreases were related to increasing section stiffness by strengthening techniques with welding used in specimens No.2 and No.3. While in specimen No. 4 (CACB2C-rLG0%), no value of deflection appeared at the level of the ultimate load of the reference specimen because of the negative effectiveness of unwelded.

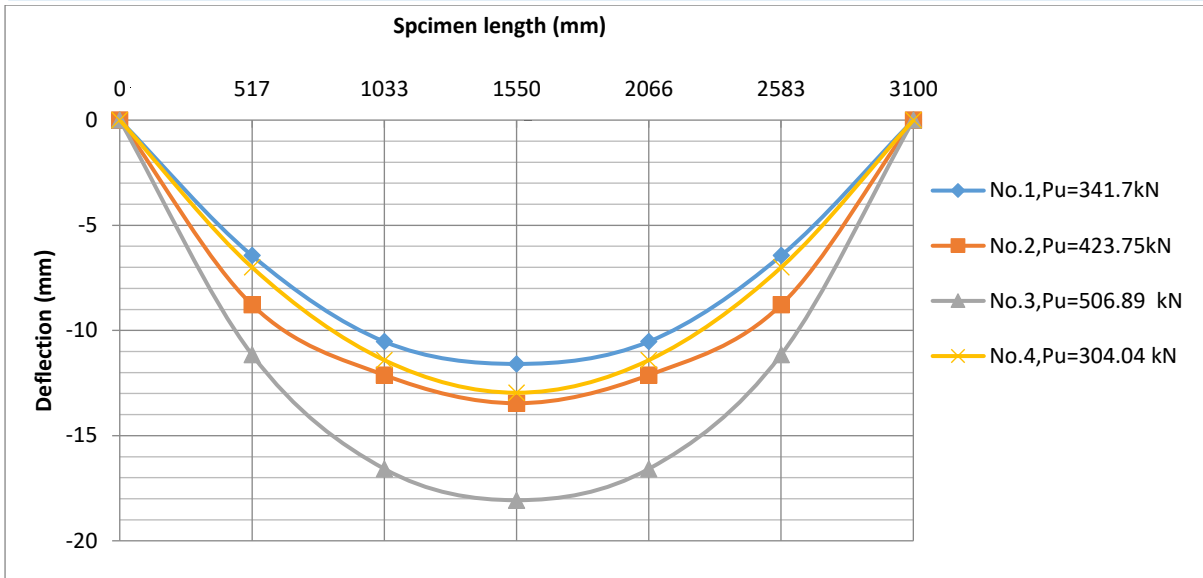


**Fig. 15** Load-Deflection Curve at Ultimate Load for All Specimens Along Specimen Length.

**Table 6** Ultimate Load and Mid-Span Deflection Values for All Specimens.

Spec. No.	Spec. Symbol	$P_u$ (kN)	$\Delta_u$ (mm)	$\frac{P_u - P_{u,ref.}}{P_{u,ref.}} \times 100\%$	$\frac{\Delta_u - \Delta_{u,ref.}}{\Delta_{u,ref.}} \times 100\%$
1	CACB2C/R	341.70	12.26	-	-
2	CACB2C-r	423.75	13.16	+24.01	7
3	CACB2C-rL	506.89	18.07	+48.34	47
4	CACB2C- rLG0%	304.04	12.96	-11.02	5.7

Where  $P_u$ =Ultimate Load,  $\Delta_u$ = Mid-span deflection at ultimate load,  $P_{u,ref.}$ = Ultimate Load for reference specimens (No.1), and  $\Delta_{u,ref.}$ = Mid-span deflection at ultimate load for reference specimen (No.1).

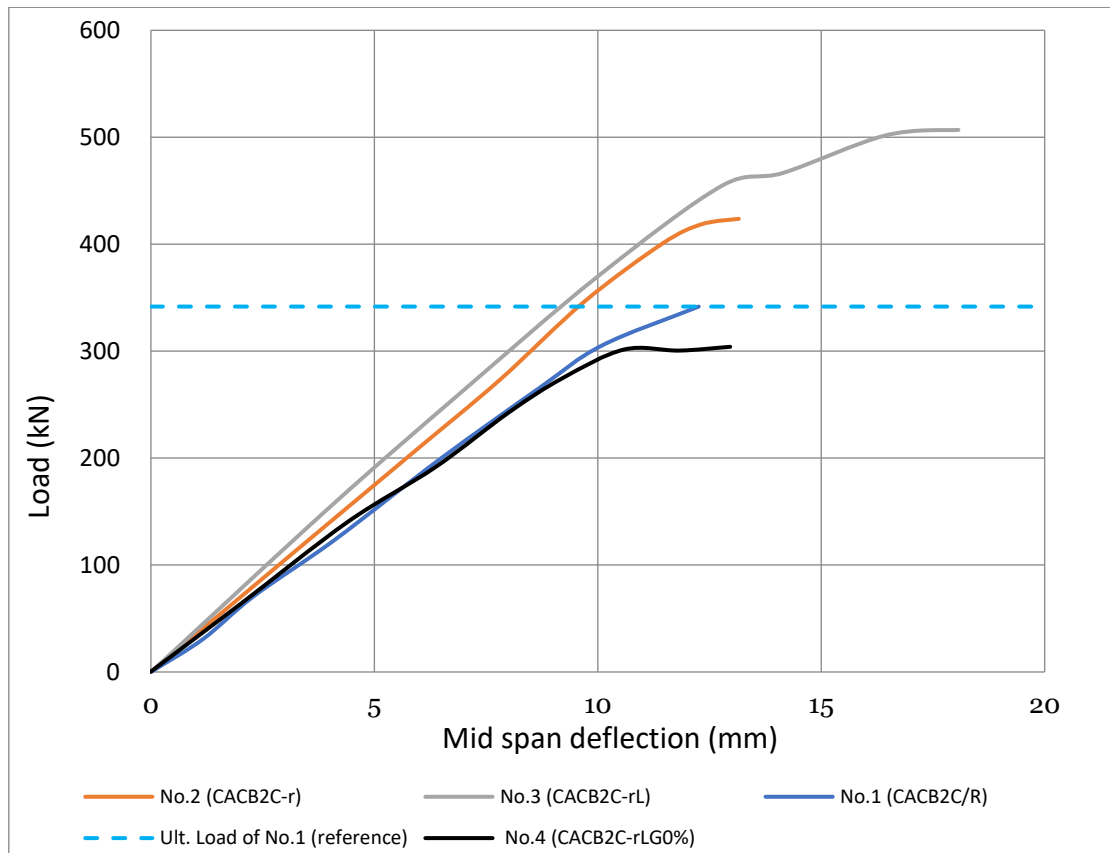


**Fig. 16** Load-Deflection Curves for All Specimens at Mid-Span.

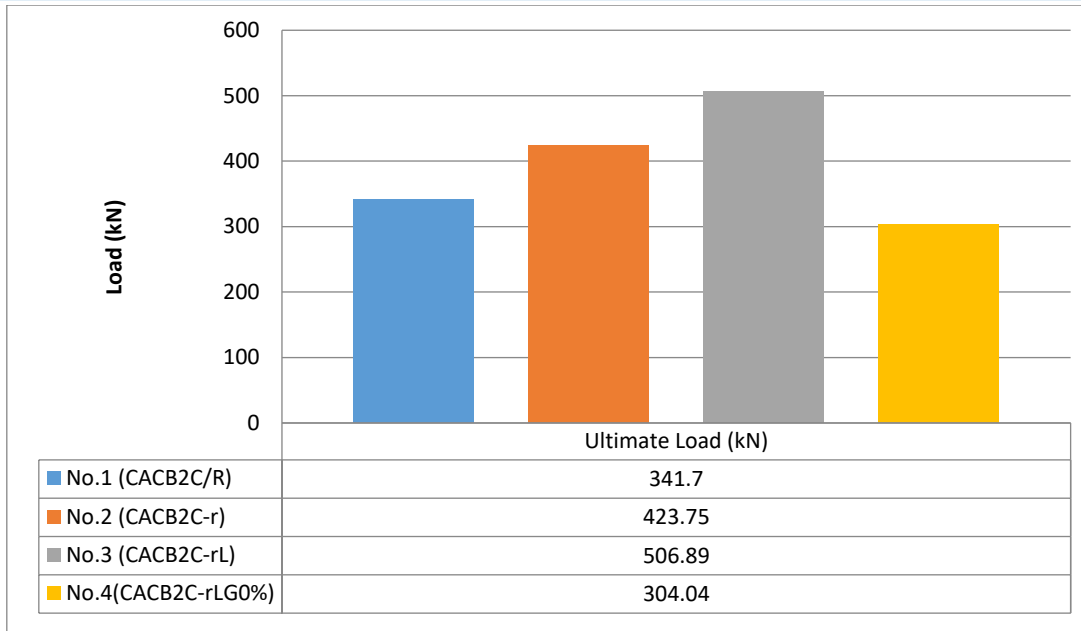


**Fig. 17** Ultimate Loads for All Specimens.

**Table 7** Deflection for Specimens Measured at the Ultimate Load of Reference Specimen No.1.

Spec. No.	Spec. Symbol	Deflection measured at ult. load of the reference beam (mm)	Difference in deflection (%)
1(Ref.)	CACB2C/R	12.69	—
2	CACB2C-r	9.69	-20.96
3	CACB2C-rL	9.21	-24.87
4	CACB2C-rLG0%	—	—

**3.2. Stiffness**

Stiffness is the load demanded to result in unit deflection. It was prepsened from deflection and ultimate load values [17]. The results showed that there was a difference in stiffness between specimens Nos. 2, 3, and 4 compared with reference specimen No. 1 of about +15.5%, +0.6%, and -15.8%, respectively, due to increasing section dimension and rigidity after the strengthening techniques, as well as a decrease in stiffness for specimen No. 4 due to

the effect of not welding in web post regions and the inability of strengthening by RPC and lacing to replace welding. Stiffness values are shown in Table 8 and Fig. 18.

**Table 8** Stiffness of Specimens.

Spec. No.	Ult. load $P_u$ (kN)	$\Delta_u$ (mm)	Stiffness= $P_u / \Delta_u$ (kN/m)	Difference in Stiffness %
1	341.71	12.26	27.87	—
2	423.75	13.16	32.19	+15.5
3	506.89	18.07	28.05	+0.6
4	304.04	12.96	23.45	-15.8

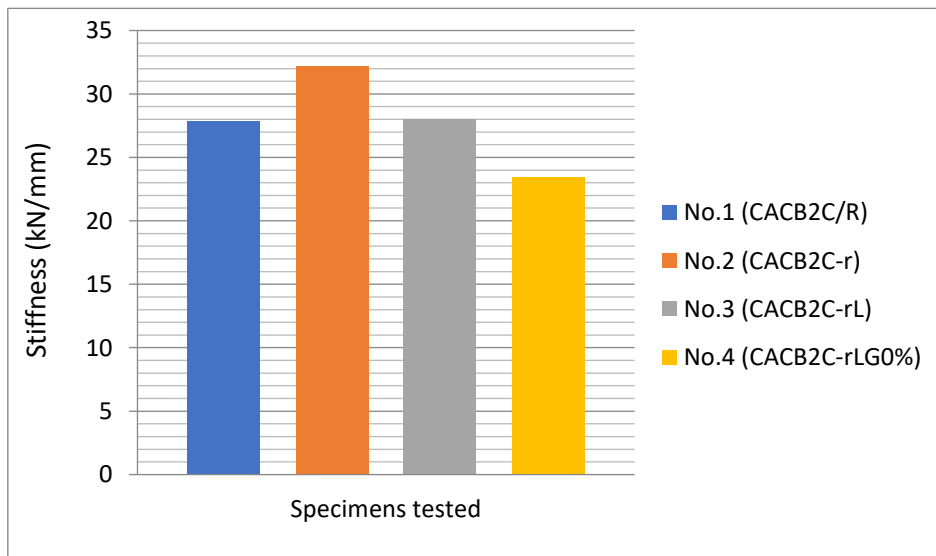


**Fig. 18** Stiffness Values for All Specimens.



### 3.3. Ductility Characteristics

Ductility is a member's ability to endure inelastic deformations after yield deformation without losing its load-carrying capacity. The ratio of the deflection at the failure to the first yield deflection is the ductility factor ( $\mu$ ) as expressed in Eq. (1):

$$\mu = \Delta u / \Delta y \quad (1)$$

where  $\Delta u$  = mid-span deflection at ultimate load, and  $\Delta y$  = mid-span deflection at first yield [18]. Fig. 19 and Table 9 shows the ductility factor results at mid-span deflection values at yield and ultimate loading stage for all specimens tested. The result showed that the ductility factor increased by 34.53% and 42.44% for spec. No.2 and No.3, respectively. This enhancement is related to using RPC and laced reinforcement that significantly increased flexural elements. In contrast, the ductility factor was decreased by 2.87% for spec. No3 compared to reference spec. No1 due to the negative effect of not welding in web post regions.

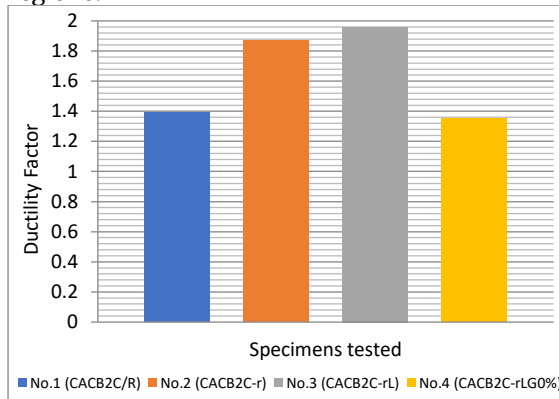


Fig. 19 Ductility Factor for Tested Specimens.

Table 9 Ductility Factor for Tested Specimens.

Spec. No.	Yield defl. $\Delta_y$ (mm)	Ult. defl. $\Delta_u$ (mm)	Ductility factor $\mu = \Delta_u / \Delta_y$	Difference in Ductility %
1	8.77	12.26	1.39	—
2	7.02	13.16	1.87	+34.53
3	9.12	18.07	1.96	+42.44
4	9.53	12.96	1.35	-2.87

Table 10 Energy Absorption Capacity for Tested Specimens.

Spec. No.	Energy Absorption Capacity kN.mm	Difference in Energy Absorption Capacity %
1	2311.75	—
2	2731.27	+18.14
3	5381.13	+132.77
4	2475.25	+7.07

### 3.4. Energy Absorption Capacity

Energy absorption capacity was calculated from the load-deflection curve [17]. The area under the load-deflection curve was considered in this study. Table 10 and Fig. 20 show the energy absorption capacity results for the tested specimens. It was found that the strengthening specimens Nos. (2-4) were increased by about 18.14 %, 132.77%, and 7.07%, respectively, compared to reference spec. No1 (without strengthening). It was noted that specimen No.3 had a more significant energy absorption capacity due to its strengthening with RPC and lacing with welding in web post regions. In contrast, specimen No.4 had a smaller energy absorption capacity due to its strengthening without welding in web post regions.

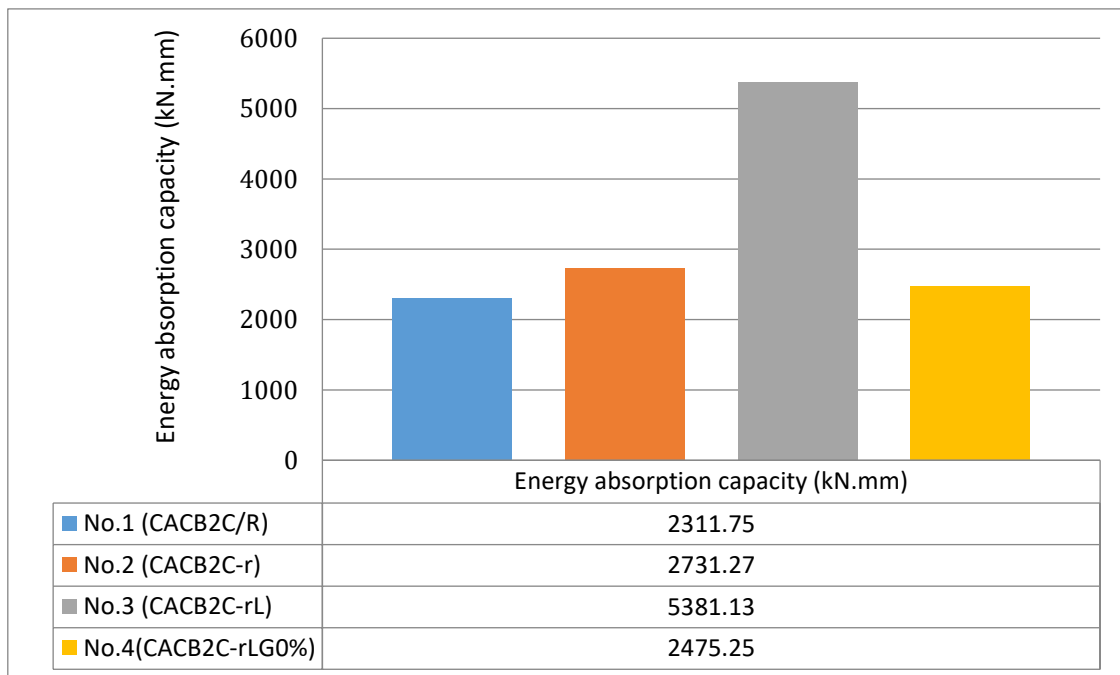


Fig. 20 Energy Absorption Capacity for Tested Specimens.

### 3.5.Failure Modes

In the present investigation, because of the rigidity provided by the concrete deck slab, the failure due to the lateral torsional buckling did not occur. Also, the failure modes, i.e., the welded joints ruptured and the slip between the deck slab and steel castellated beam, were ruled out as they were correctly designed. For all tested specimens, the modes of failure and the first crack are illustrated in Table 11. The initial failure mode that occurred for all examined specimens was flexural failure mode due to the response of composite beams to away imposed concentrated Loads directly on castellated openings. The reference specimen No.1 had a flexural failure and yielding in the bottom flange near the support because it was the weakest section due to its smaller thickness, i.e., 9.9mm, compared to the web thickness, i.e., 15.38 mm (double channel), the existence of welding strength in web post locations, and the strengthening lack in the web area, see Fig. 21. In contrast, specimen No.2, which was strengthened with only RPC, showed flexural failure, and the web post local buckling failure obviously close support resulted in a lateral lunge to the RPC development of evident cracks in the form of shear mode failure, see Fig. 22. For specimen No.3, which strengthened with RPC and Lacing, the mode failure began with flexural, then yielded in the bottom flange, i.e., its weakest region, compared to the strength web with RPC and Lacing. After that, the failure was trans into a crash in the concrete deck slab, and after that, cracks appeared on the RPC surface near the support represented by shear mode failure, see Fig. 23. Finally, in Fig. 24, specimen No. 4 was strengthened by RPC and lacing without welding in web post regions. The failure mode began with flexural, and because there was no welding, the web pushed out the RPC by side with shear failure mode and yielding mode in the bottom flange, then local buckling happened in the top flange, resulting in crashing mode in the concrete deck slab.

**Table 11** Failure Modes and First Crack for Experimentally Tested Specimens.

Spec. No.	First Crack Load (kN)	Failure Mode
1	–	Flexural and yielding in the bottom flange.
2	110	Flexural, local buckling in the web and shear.
3	100	Flexural, yielding in the bottom flange, local buckling in the top flange, and crushing in the concrete deck slab and shear.
4	90	Flexural, yielding in the bottom flange, shear, local buckling in the top flange, and crushing in the concrete deck slab.



**Fig. 21** The Failure Mode for Specimen No.1.

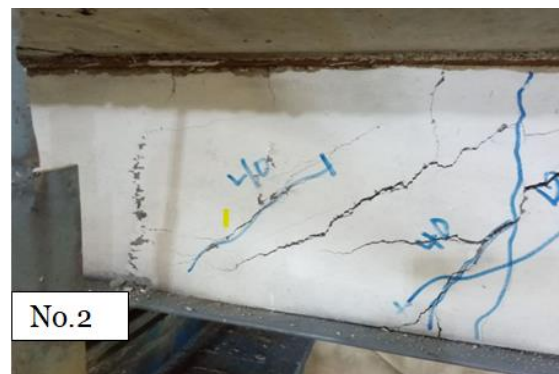


**Fig. 22** The Failure Mode for Specimen No.2.





Fig. 23 The Failure mode for specimen No.3.

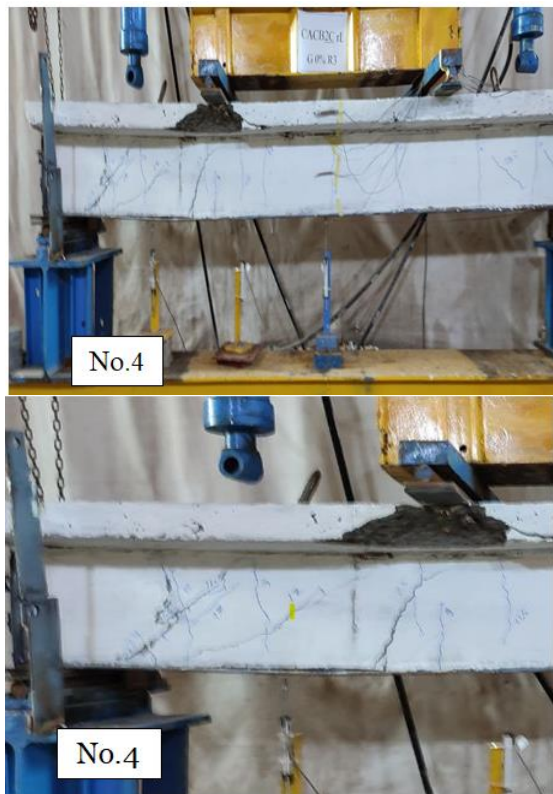


Fig. 24 The Failure mode for specimen No.4.

#### 4. CONCLUSIONS

The main conclusions of the experimental results obtained from this study are the following:

- 1- A reduction in the deflection for strengthening specimens at the loading level (the reference specimen's deflection at maximum load).

- 2- Compared to the reference specimen (welding without strengthening), there was an increase in the ultimate load capacity for strengthening welding specimens (used RPC in the web without and with lacing) by 24.01% and 48.34%, respectively. The ultimate load capacity decreased by roughly 11.02% when the unwelded specimen was strengthened with RPC and lacing compared to the reference specimen.
- 3- A larger energy absorption capacity was found in the specimen strengthened with RPC and lacing with welding in web posts. In comparison, the specimen that strengthened with RPC and lacing without welding in web posts had a smaller energy absorption capacity.
- 4- The welding operations in the areas of web posts of castellated steel sections cannot be compensated by replacing them with RPC and lacing.
- 5- All specimens began to fail in the flexural mode to make a system consisting of RPC, Lacing, and welding work relatively, then went to other failure modes and occurred differently.
- 6- Increasing the net openings span is possible compared with a reference castellated specimen.

#### ACKNOWLEDGEMENTS

The authors thank the Civil Engineering Department-University of Baghdad/Iraq for their support.

#### REFERENCES

- [1] Fares S, Coulson J, Dinehart D. **Castellated and Cellular Beam Design**. 14<sup>th</sup> ed., USA: American Institute of Steel Construction; 2016.
- [2] Knowles PR, 5950 BS. **Castellated Beams**. *Proceedings of the Institution of Civil Engineers* 1991; **90**(3):521-536.
- [3] Larnach J, Park R. **The Behavior under Load of Six Castellated Composite T-Beams**. *Civil Engineering and Public Works Review* 1964; **59**(692):339-343.
- [4] Kumar VS, Nandhakumar P, Indrajit M, Swathika P. **Research on Structural Behavior of Concrete Encased Steel Castellated Beam for Different Sections**. *International Journal of Engineering and Advanced Technology* 2019; **8**(6): 61-64.
- [5] Hadeed SM, Alshimmeri AJH. **Comparative Study of Structural Behaviour for Rolled and Castellated Steel Beams with Different Strengthening Techniques**. *Civil Engineering Journal* 2019; **5**(6):1384-1394.
- [6] Ridha MM, Sarsam KF, Al-Shaarbaf IA. **Experimental Study and Shear**



- Strength Prediction for Reactive Powder Concrete Beams.** *Case Studies in Construction Materials* 2018; **8**:434-446.
- [7] Qasim OA. **Comparative Study between the Cost of Normal Concrete and Reactive Powder Concrete.** *IOP Conference Series: Materials Science and Engineering* 2019; **518**: 022082, (1-15).
- [8] Ali AH, Ibrahim AK. **Mechanical Properties of Reactive Powder Concrete (RPC) Exposed to Acidic Solutions.** *Tikrit Journal of Engineering Sciences* 2014; **21**(3):55-62.
- [9] Ammar HA, Alshimmeri AJH. **A Comparison Study between Asymmetrical Castellated Steel Beams Encased by Reactive Powder Concrete with Laced Reinforcement.** *Key Engineering Materials* 2021; **895**:77-87.
- [10] Khaleel AI, AL-Shamaa MF. **Experimental Investigation on the Structural Behavior of Double Channel Castellated Steel Beams.** *E3S Web of Conferences* 2021; **318**: 03009, ().
- [11] Al-Tameemi SK, Alshimmeri AJ. **Behavior of Asymmetrical Castellated Composite Girders by Gap in Steel Web.** *AIP Conference Proceedings* 2023; **2414**(1): 060002, (1-11).
- [12] AISC AISC. *Steel Construction Manual*. 15th Edition ed. Chicago, Illinois; 2017.
- [13] Al-Thabthabee HW. **Experimental Study of Effect of Hexagonal Holes Dimensions on Ultimate Strength of Castellated Steel Beam.** *Kufa Journal of Engineering* 2017; **8**(1): 97-107.
- [14] ASTM A. *A615 Standard Specification for Deformed and Plain Carbon-Steel Bars for Concrete Reinforcement*. ASTM International, West Conshohocken, PA 2016.
- [15] Abbas AN. **Experimental Study on Reactive Powder and Normal Concrete Rectangular Beams under Different Loading Rate.** *International Journal of Engineering and Advanced Technology Structures* 2014; **2**(2): 1-10.
- [16] Iraqi Standard Specification No.45. for Aggregate from Natural Sources for Concrete and Building Construction. Central Organization for Standardization and Quality Control, Baghdad, Iraq, P11 1984.
- [17] Ahmad S, Masri A, Abou Saleh Z. **Analytical and Experimental Investigation on the Flexural Behavior of Partially Encased Composite Beams.** *Alexandria Engineering Journal* 2018; **57**(3):1693-1712.
- [18] Hallawi AF, Al-Ahmed AHA. **Enhancing the Behavior of One-Way Reinforced Concrete Slabs by Using Laced Reinforcement.** *Civil Engineering Journal* 2019; **5**(3):718-728.